Modelling the dynamics of the electron transport rate measured by PAM fluorimetry during Rapid Light Curve experiments

J.-M. GUARINI[*,**] and C. MORITZ[*,**]

Université Pierre et Marie Curie, Paris 6, CNRS; UMR7621, Laboratoire d'océanographie biologique de Banyuls, Avenue Fontaulé, BP44, F-66650 Banyuls-sur-Mer, France[*]
Université Pierre et Marie Curie, Paris 6, CNRS; UMR7625, Laboratoire d'écologie, biodiversité et évolution, Quai Saint-Bernard, F-75005 Paris, France[**]

Abstract

We propose a dynamic model specifically designed to simulate changes in the photosynthetic electron transport rate, which is calculated from fluorescence measurements when plants are exposed, for a short time, to a series of increasing photon flux densities. This model simulates the dynamics of the effective yield of photochemical energy conversion from the maximum and natural chlorophyll fluorescence yields, taking into account a cumulative effect of successive irradiations on photosystems. To estimate a characteristic time of this effect on photosystems, two series of experiments were performed on two benthic diatom culture concentrations. For each concentration, two different series of irradiations were applied. Simplified formulations of the model were established based on the observed fluorescence curves. The simplified versions of the model streamlined the parameters estimation procedure. For the most simplified version of the model (only 4 parameters) the order of magnitude of the characteristic time of the residual effect of irradiation was about 38 s (within a confidence interval between 20 and 252 s). The model and an appropriate calibration procedure may be used to assess the physiological condition of plants experiencing short time-scale irradiance changes in experimental or field conditions.

Additional key words: diatom; photosystem; photosynthesis.

Introduction

Fluorescence kinetics is measured to study the photosynthetic performances of plants (Dau 1994). The short-term modifications of photosystem 2 (PSII) during changing irradiance are useful indicators of the

Received 20 February 2008, *accepted* 12 October 2008.
Fax: (+33) 4 68 887 395, e-mail: guarini@obs-banyuls.fr

Abbreviations: The symbol "^", which caps a constant, a matrix or a vector, signifies "estimated"; N is a set of natural integer numbers, R is a set of real numbers; *means 0 excluded. Many variables and constants are dimensionless.
a − multiplication coefficient of I in the function δ(I) [m^2 μmol^{-1}(photon)]; b − exponent of I in the function δ(I); Chl – chlorophyll; COV − variance-covariance matrix; E_t − PFD received by the plant at the time t [μmol(photon) m^{-2} s^{-1}]; ETR – electron transfer rate between photosystems I and II; ETR_{max} − maximum value of ETR during one RLC or LC experiment; F, f – fluorescence yield in the ambient irradiance environment; F_m – dark adapted maximum fluorescence yield; F_0 – dark-adapted minimum fluorescence yield; F_0' – minimum fluorescence yield during irradiation; g − the rate of convergence between M and F [s^{-1}]; I(t) = I − integrated photon accumulation by the plant [μmol(photon) m^{-2}]; i, j, q, r − indices. i,j,q,r ∈ N^{*4}; J − the Jacobian matrix of Y_t, described by r parameters p; J^T − transposed matrix of J, $[J^TJ]^{-1}$ is the inversed matrix $[J^TJ]$; k − the rate of attenuation of the residual light effect [s^{-1}]; LC – light curve ; M – the fluorescence yield reached during the saturation pulse; M_{min} – minimum fluorescence yield reached during saturation; m, n − numbers of consecutive times defining the series of light exposure E_t; n_q − numbers of experimental fluorescence data for the models q, q = 1 … Q; p − numbers of parameters to estimate, p ∈ N^*;. p_1, p_2, p_3, p_4 − parameters describing the simplified dynamics of Y; PE – photosynthesis-irradiance curve; PFD – photon flux density; Q − number of models; RC – rebuilt curve; RLC − rapid light curve; s^2 − the sum of the square residuals (ε^2) divided by (n − p); t – forward time [s]; Δt − discrete time step [s]; Y – the effective yield of photochemical energy conversion [at t, $Y_t = (1 - F/M)_t$]; β − the absorption factor of the plant [m^2 μmol^{-1}(photon)]; δ(I) − function describing the effect of I(τ) on the dnamics of M, F, and Y; θ_I − vectors (or set) of parameters describing δ(I) in dynamics of F, M, and Y; θ_F − vectors (or set) of parameters describing the dynamics of F; θ_M − vectors (or set) of parameters describing the dynamics of M; θ_Y − vectors (or set) of parameters describing the dynamics of Y; Φ, ψ − criteria functions used in optimisation processes; τ – backward time [s]; φ_F − the integrated function describing the dynamics of F; φ_M − the integrated function describing the dynamics of M; φ_Y − the integrated function describing the dynamics of Y.

Acknowledgments: We thank Ms. Jennifer Coston-Guarini for having revised the manuscript, commented on the approach, and inspired discussion about optimisation.

physiological state of plants (Horton and Ruban 2004) and Pulse Amplitude Modulated (PAM) fluorimetry, which measures fluorescence in natural or artificial ambient irradiances (Schreiber *et al.* 1986, 1994, Kolber and Falkowski 1993), is well-adapted to monitoring PSII activities. PAM fluorimetry offers the possibility to investigate the photosynthetic yield (Schreiber *et al.* 1986, Genty *et al.* 1989) of plants submitted to fluctuating photon flux densities (PFD).

During a fast dark/light transition, effective yield and the electron transfer rate have a transitory phase called the "Kautsky effect", which provides information about the electron transport reactions through PSII (Lichtenthaler 1992). Experiments in which the overall plant environment is controlled, and during which rapid variations of photon flux density are induced, lead to "Rapid Light Curve" estimates. RLC are used to study the physiological flexibility of plants' photosynthetic units to rapid changes in irradiation, similar to what occurs in natural environments (Schreiber *et al.* 1997, White and Critchley 1999, Ralph and Gademann 2005). They provide detailed eco-physiological information on photosynthetic performances of plants as a function of their physiological condition (Wing and Patterson 1993, Kubler and Raven 1996, Hewson *et al.* 2001, Seddon and Cheshire 2001).

The relationship between the Electron Transport Rate (ETR) and PFD is usually represented by an autonomous (*i.e.* time independent) function (Kühl *et al.* 2001, Longstaff *et al.* 2002, Campbell *et al.* 2003, Figueroa *et al.* 2003, Ralph and Gademann 2005, Serôdio *et al.* 2006). The resulting ETR *vs*. PFD curves are transposed from photosynthesis *vs.* irradiance (P-E) curves, which were formulated for carbon production estimated from ^{14}C assimilation experiments (Frenette *et al.* 1993). However, such mathematical formulations are not appropriate to simulate ETR variations for two reasons: (*1*) The ETR estimates at the time t are calculated by a linear multiplication of the PFD, E_t, with an effective yield of photochemical energy conversion, Y_t. Therefore, it is not possible to represent ETR_t *vs.* E_t, with non-linear P-E curve formulations, which requires that ETR_t substitutes for $P(E_t)$ in the equation. (*2*) Furthermore, Y_t is a function of M, the fluorescence yield reached by the saturation pulses, and F, the natural fluorescence yield (*i.e.* yield in the ambient irradiation), which are both dynamic processes (Schreiber *et al.* 1997, Johnson 2000). Hence, an autonomous function that represents a steady state process (in which time does not intervene), cannot simulate variations of ETR_t.

A dynamic model that represents the kinetics of the effective yield, Y(t), can solve these two problems, and should allow proper simulations of ETR(t) between PSII and PSI. The objective of this paper is to formulate such a dynamic model, with a perspective of using it in physiological or eco-physiological studies using fluorescence measurements to investigate photosynthetic properties of plants. Simplifications of the model and calibration procedures are also proposed to make the model operational and accessible to other researchers in the field.

Materials and methods

Methods, assumptions and model*:* ETR represents the rate at which electrons are transferred from PSII to PSI. It is calculated from a series of fluorescence yields measured at each experimental time, t $\{t = t_1,\ldots,t_n\}$ as:

$$ETR_t = 0.5\beta\left(1-\frac{F}{M}\right)_t E_t \qquad (1)$$

where 0.5 expresses equal excitation energy distribution between PSII and PSI, β is the absorption factor of the plant sample, M is the fluorescence yield reached during the saturation pulse, F is the natural fluorescence yield (*i.e.* yield in the ambient iradiation), and E_t is the PFD received by samples at the time t. The function $Y_t = (1 - F/M)_t$ represents the effective yield of photochemical energy conversion at the time t (Genty *et al.* 1989).

RLC are recorded by applying a series of n rapidly increasing PFD to the same plant sample, corresponding to n consecutive times t, $\{t=t_1,\ldots,t_n\}$. At the beginning of the experiment, plant samples are dark-adapted, in such a way that $F = F_0$ and $M = F_m$. As soon as a previously dark-adapted sample receives photons, the effective yield of photochemical energy conversion, Y, decreases due to the modification in the PSII configuration. M decreases, while F converges asymptotically to M. In terms of photochemistry, photochemical quenching decreases while non-photochemical quenching increases. Y depends on the way that the plant sample reacts to a given variable irradiation regime. According to the experimental conditions of RLC measurements, variables F and M are functions of time and depend on the short irradiation history of the plant (Schreiber *et al.* 1997) which can be seen as a cumulative effect of irradiation on photosystems with respect to their short term irradiation history. In other words, fluorescence yields depend not only on the irradiation of the plant sample at the moment of the measurement, but also on its past exposures. A function I(t) was defined to describe this cumulative effect, which is assumed to attenuate (*i.e.* it decreases) exponentially with a backward-looking (retrospective) time, τ, $\tau \leq t$:

$$I(t) = \int_0^t e^{k(\tau - t)} E(\tau) d\tau \qquad (2)$$

This formulation is minimal; the strength of the effect is only described by one parameter, k (in $time^{-1}$) which is a linear rate of attenuation. 1/k can be interpreted as a characteristic time of residual photon accumulation. The integral represents the cumulative effect from the beginning of the experiment to each experimental time t, at which fluorescence yields were actually measured. At

$t = t_0$, plants are considered to be dark-adapted, and initial conditions are $E_0 = 0$, and $ETR_0 = 0$.

The calculation of ETR (Eq. 1) can be re-written as:

$$ETR_t = ETR_t = 0.5\beta\left(1 - \frac{F(I)}{M(I)}\right)_t E_t = 0.5\beta(Y(I))_t E_t$$

and the continuous dynamic system describing changes in F and M was formulated as:

$$\begin{cases} \dfrac{dM}{dI} = -(M - M_{min})\delta(I,\theta_I) \\ \dfrac{dF}{dI} = g(M - F) - (M - M_{min})\delta(I,\theta_I) \end{cases} \quad (3)$$

where M_{min} is the minimal fluorescence yield for M, $\delta(I,\theta_I)$ a function representing the variation rate of M as a function of I(t)—written I for sake of simplification, and g (in time^{-1}) is a rate of convergence between F and M. Variations of M are independent from variations of F. Conversely, M controls the variations of F. This is consistent with the definition of M, which represents the fluorescence during a saturating pulse of photons, and thus depends only on its own previous values, but not on the value taken by F. On the contrary, the difference between F and M (which is the consequence of the difference between the ambient irradiation and the saturation irradiance) was taken into account to calculate variations of F.

This system (Eq. 3) has to respect the following three conditions:

$$\begin{aligned} &(a)\ F_m \geq M \geq M_{min} \geq F_0' \\ &(b)\ M \geq F \\ &(c)\ g\,(M - F) \geq (M - M_{min})\,\delta(I,\theta_I) \end{aligned} \quad (4)$$

The function $\delta(I,\theta_I)$, which describes the variation rate of M, was formulated as:

$$\delta(I,\theta_I) = a\, I^b \quad (5)$$

The vector of parameters $\theta_I = \{(a, b) \in R^+ x\ R^+\}$ needs to be estimated from experimental data. As I is always positive or equal to zero, $\delta(I,\theta_I)$ remains always positive or equal to zero [M decreases when the sample is maintained to irradiation, and $\delta(I,\theta_I)$ increases when I increases]. This formulation is sufficient for RLC experiment. However, for a more general purpose (experiments including re-adaptation to dark), the term $-(F_m - M)\ \delta_0$ should be added to the equations (system 3), with $\delta_0 \in R^+$ is a rate of recovery. The ordinary system of differential Eq. (3) with initial conditions $M(0) = F_m$, and $F(0) = F_0$ can be solved analytically, to calculate Y_t and ETR_t, but requires the numerical evaluation of complex integrals.

Parameter estimates and simplification of the formulation: The system of Eq. (3) was simplified by considering that the variations of F were small compared to the variations of M (which thus became the only variable to control the fluctuations of the effective yield of photochemical energy conversion, Y). This simplification implied that, with respect to condition of Eq. 4c (above), $g(M - F) \approx M\delta(I)$. Then, $dF/dt \approx 0$ and F is fixed as a constant, f. The simplified function describing $\varphi_Y(I_t,\theta_Y)$ is:

$$\varphi_Y(I_t,\theta_Y) = 1 - \frac{F_t}{M_t} = \frac{p_1 + e^{(-p_3 I_t p_4)}}{p_2 + e^{(-p_3 I_t p_4)}} \quad (6)$$

with $p_1 \in R^*$ and $(p_2,p_3,p_4) \in R^{+*} x\ R^{+*} x\ R^{+*}$. These were the parameters to be estimated by minimisation of the criteria function. Optimal values of $\theta_Y = \{p_1,p_2,p_3,p_4\}$ were estimated directly on calculated data describing the relationship ETR *vs.* E_t. The optimisation consists of fitting curves, $Y = \varphi_Y(I,\theta_Y)$. More weight was given to the values calculated with a higher E_t, since the minimization of an ordinary least square criterion uses weights which are proportional to the square of the E_t values. The criterion function Φ is indeed:

$$\Phi = \min \sum_{t=t_0}^{t_n} \left(0.5\beta E_t \left(\varphi_Y(I_t,\hat{\theta}_Y) - Y_t\right)\right)^2 \quad (7)$$

and the weights are equal to $(0.5\ \beta\ E_t)^2$. When two curves are available, a revised optimisation process was performed on ETR curves in two nested steps, to include estimate of the parameter k:

Step 1. The parameter k, was estimated from two ETR curves (with two different light histories represented by $I_{ti}(k)$ and $I_{tj}(k)$), ETR1, with n_1 measurements, and ETR2, with n_2 measurements. A direct search algorithm (*Simplex*; Nelder and Mead 1965) minimized the overall distance between the two fitted curves. The following criteria function was used:

$$\psi = \min\left[\sum_{i=1}^{n_1} \left(\left(\varphi_{Y1}(I_{ti},\hat{\theta}_{Y1}) - \varphi_{Y2}(I_{ti},\hat{\theta}_{Y2})\right)0.5\beta E_{ti}\right)^2 + \sum_{j=1}^{n_2} \left(\left(\varphi_{Y1}(I_{tj},\hat{\theta}_{Y1}) - \varphi_{Y2}(I_{tj},\hat{\theta}_{Y2})\right)0.5\beta E_{ti}\right)^2\right] \quad (8)$$

Step 2. The two sets of parameters $\hat{\theta}_{Y1} = \{p_1,p_2,p_3,p_4\}_1$ and $\hat{\theta}_{Y2} = \{p_1,p_2,p_3,p_4\}_2$ were estimated at each iteration (step 1) using the same direct search algorithm, which minimized the criteria function, Φ (Eq. 6).

In the final step, the variance-covariance matrix of the parameters $\{\hat{k}, \hat{p}_1, \hat{p}_2, \hat{p}_3, \hat{p}_4\}$ was estimated using a linear approximation of the solutions around the best. J represents the Jacobian matrix of Y_t, and s^2, the sum of square residuals divided by n-p degree of freedom (where p is the number of parameters to estimate). The variance-covariance matrix of $\hat{\theta}_Y$ was then calculated as:

$$\hat{COV}(\hat{\theta}_Y) = s^2\left[J^T J\right]^{-1}$$

Experimental design. In order to apply the model to actual data, experiments were performed with benthic microalgal biofilms (Consalvey *et al.* 2004). Benthic

unicellular microalgae form a biofilm at the marine or freshwater sediment surface and are easy to collect and manipulate experimentally (Blanchard *et al.* 1997). This biofilm does not exhibit the spatial variabilities of fluorescence and effective yield efficiency which have been reported over leaf surfaces or between other multicellular plants (Nedbal *et al.* 2000). For these experiments, benthic microalgae, mainly pennate diatoms, were collected at the surface of a marine intertidal mudflat, extracted from the sediment using active vertical migration, and suspended in GF/F filtered seawater (see Blanchard *et al.* 1997 for details about the experimental protocol).

Fluorescence data were recorded with a PAM fluorometer (Diving-PAM, *H. Walz*, Effeltrich, Germany). Two suspensions of benthic diatoms in filtered seawater (at two different concentrations) were used to re-create biofilms by sedimentation in vials. Biofilms were created in flat-bottom vials with a 1.5 cm diameter that matched the diameter of the PAM fluorometer optic fibre used. The optic fibre was placed precisely at 1 cm from the biofilm. Three cm^3 aliquots of the prepared suspensions were introduced into each vial, in order to recreated biofilms containing in average 36 mg(Chl *a*) m^{-2} and 53 mg(Chl *a*) respectively. Measurements of Fluorescence were replicated four times at each light intensity, and each set $\{F_0', F, M\}$ of four fluorescence replicates were averaged to reduce heterogeneities due to the variability of the mass of Chl *a* in the biofilms. Measurements of chlorophyll a concentrations were replicated four times, at the end of each experiment, and were performed using the Lorenzen method (Lorenzen 1966)

Before each experiment, samples were dark-adapted for 1 800 s. A first series of RLC was done for each sample by increasing, progressively, the PFD every 50 s [$\{t_i=t_1,\ldots,t_n\}$, $n = 12$ consecutive times)]. Therefore, during $\Delta t = 50$ s, the irradiance E_{ti} was constant. I_t, at each time t_m ($1 \le m \le n$) was calculated analytically by:

$$I_{t_m} = \int_0^{t_m} e^{k(\tau - t_m)} E(\tau) d\tau = \sum_{i=1}^{m} \left(E_{t_i} \int_{t_i - \Delta t}^{t_i} e^{k(\tau - t_i)} d\tau \right) =$$

$$= \sum_{i=1}^{m} \left(E_{t_i} \left(\frac{1 - e^{-k\Delta t}}{k} \right) \right) \quad (9a)$$

When no residual effect of irradiation is assumed, the parameter k is set to 1 s^{-1}, which is high enough to ensure that, at our scale of measurements, $I_t \approx E_t$. The parameter k [s^{-1}] was estimated from two RLC with two different irradiation histories. A second series of RLC experiments were completed for each biofilm concentration (using the same protocol), except that at each time t $\{t = t_1,\ldots t_n\}$, every 50 s, a new dark-adapted sample, maintained in darkness since t_0, was exposed suddenly to a new E_t. The series of E_t values were the same as in the previously described experiment, except that each plant sample had a different irradiation history. This second experiment was referred as rebuilt curve (RC). The calculation for I_t at each time t_m, ($1 \le m \le n$), became:

$$I_{t_m} = \int_0^{t_m} e^{k(\tau - t_m)} E(\tau) d\tau = E_{t_m} \int_{t_m - \Delta t}^{t_m} e^{k(\tau - t_m)} d\tau =$$

$$= E_{t_m} \left(\frac{1 - e^{-k\Delta t}}{k} \right) \quad (9b)$$

Results and discussion

Conditions of calculations and parameters estimates: The preliminary tasks consisted of testing the relevance of the dynamic behaviour of the system. Measurements of the fluorescence yields showed that the overall variations of F were small compared to variations of M (Fig. 1), legitimating simplifications of the model (Eq. 6). The strongest variations in F were recorded for low PFD exposures. In addition, ancillary fluorescence measurements were made during each of the two experiments (Fig. 1*A,B*) in order to make sure that F_0 did not show any significant changes with time (*i.e.* the moving average $\overline{F}_0$ remained constant), and that F_0' remained lower than F when F decreased below F_0.

Table 1 contains the estimated parameters $\{\hat{k}, \hat{p}_1, \hat{p}_2, \hat{p}_3, \hat{p}_4\}$ and their standard error estimates, and Table 2 contains an example of the estimated correlation coefficients between parameters. The fitted curves (*solid line*) for both biofilm concentrations are shown in Fig. 2. The model fitted well to observed ETR_t, and parameters estimates $\{\hat{p}_1, \hat{p}_2, \hat{p}_3, \hat{p}_4\}$ were strongly correlated, but the correlation coefficient estimates of $\{\hat{k}\}$ with $\{\hat{p}_1, \hat{p}_2, \hat{p}_3, \hat{p}_4\}$, although they were lower, remained around 0.35 and thus cannot be neglected. Therefore, sets of parameters must be compared separately, using an appropriate statistic for non-linear functions (Blanchard *et al.* 1997), when testing differences between fitted curves.

Parameters signification and a new simplification: The parameter that had the highest estimate uncertainties was p_1. The standard error, SE has the same order of magnitude as its corresponding best estimates. The best estimates also had the smallest value (the order of magnitude was 10^{-4}).

In Eq. (6), p_1 was calculated as:

$$p_1 = \frac{-f + M_{min}}{F_m - M_{min}}$$

which converges to 0 when M_{min} converges to f. The parameter p_2, is calculated as:

$$p_2 = \frac{M_{min}}{F_m - M_{min}}$$

and represents the standardized value of minimum fluorescence yield that can be reached during a saturation pulse, regarding to the maximum range of its variations. p_3 and p_4 are respectively equal to a and b+1, the parameters describing the variation rate of M as a function of the irradiation $\delta(I,\{a,b\})$, as it was perceived by the plant sample, hence including the cumulative effect of irradiation on the fluorescence of photosystems.

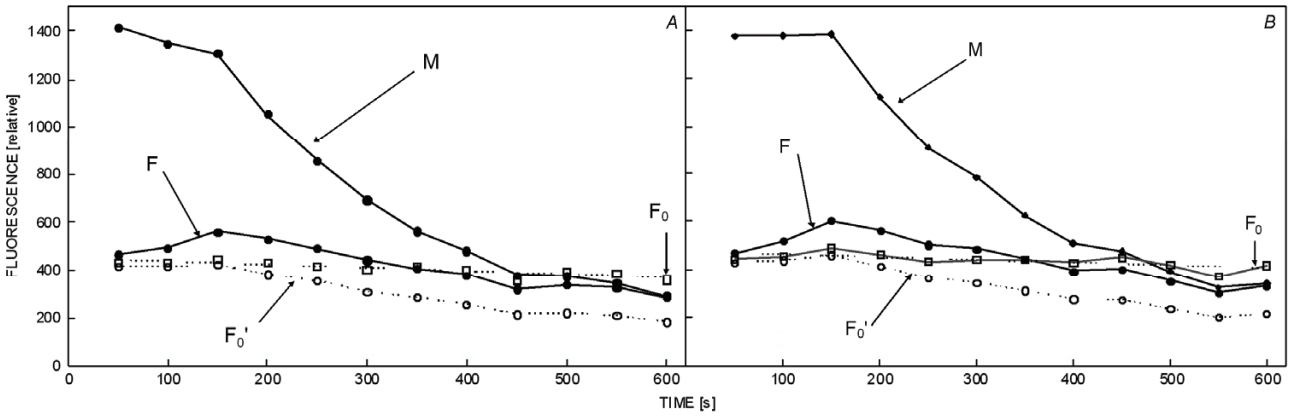

Fig. 1. The maximum fluorescence (M), minimal fluorescence (F_0'), dark-adapted minimal fluorescence (F_0), and natural fluorescence yields measured by PAM fluorimetry on a reconstructed benthic diatom biofilm. Measurements were made on independent samples maintained in dark conditions and then exposed to increasing photon flux density for 50 s. These curves were then called RC in contrast with RLC measured when the same sample was submitted to the range of increasing irradiation, with an equivalent 50 s step, and for which a control of the dark-adapted minimal fluorescence, F_0, cannot be performed. Two biofilm concentrations were investigated: (*A*) 36±5 mg(Chl *a*) m^{-2}. (*B*) 53±7 mg(Chl *a*) m^{-2}.

Table 1. Best estimates and standard errors (SE) of parameter estimates $\{\hat{k},\hat{p}_1,\hat{p}_2,\hat{p}_3,\hat{p}_4\}$ using Eq. (8) in the calculation of ETR_t. Two concentrations were investigated: (*1*) 36±5 (SD, *n*=4) mg(Chl *a*) m^{-2} and (2) 53±7 (SD, *n*=4) mg(Chl *a*) m^{-2}, and two different irradiation dynamics were applied (corresponding to RLC and RC, respectively).

	RLC – 1		Rebuilt – 1		RLC – 2		Rebuilt – 2	
	Best estimates	SE	Best estimates	SE	Best estimates	SE	Best estimates	SE
k	$2.51\ 10^{-2}$	$0.78\ 10^{-2}$	$2.51\ 10^{-2}$	$0.03\ 10^{-2}$	$2.71\ 10^{-2}$	$0.50\ 10^{-2}$	$2.71\ 10^{-2}$	$0.01\ 10^{-2}$
p_1	$2.86\ 10^{-4}$	$2.53\ 10^{-4}$	$1.19\ 10^{-4}$	$0.74\ 10^{-4}$	$6.49\ 10^{-4}$	$4.33\ 10^{-4}$	$-5.35\ 10^{-4}$	$4.76\ 10^{-4}$
p_2	$3.47\ 10^{-2}$	$0.00\ 10^{-2}$	$17.8\ 10^{-2}$	$0.00\ 10^{-2}$	$5.20\ 10^{-2}$	$0.00\ 10^{-2}$	$3.06\ 10^{-2}$	$0.00\ 10^{-2}$
p_3	$2.63\ 10^{-1}$	$0.01\ 10^{-1}$	$0.62\ 10^{-1}$	$0.00\ 10^{-1}$	$1.72\ 10^{-1}$	$0.00\ 10^{-1}$	$5.70\ 10^{-1}$	$0.06\ 10^{-1}$
p_4	$2.94\ 10^{-1}$	$0.00\ 10^{-1}$	$3.97\ 10^{-1}$	$0.00\ 10^{-1}$	$3.32\ 10^{-1}$	$0.00\ 10^{-1}$	$2.18\ 10^{-1}$	$0.00\ 10^{-1}$

Considering that the estimates of the confidence intervals (CI) are equal to the mean±1.96 SE (with SE, the square root of the estimators variance estimates), estimated values of p_1 were not significantly different from zero. Therefore, the model (Eq. 6) was simplified, assuming that $p_1 = 0$, and the optimisation procedure was repeated (Table 3). The estimated variances of the remaining parameters $\{\hat{k},\hat{p}_2,\hat{p}_3,\hat{p}_4\}$ did not increase significantly and remained low compared to the best estimated values. A significant increase in variance due to the loss of one parameter (which also corresponds to a loss of one degree of freedom) affected mainly the estimates of parameter k. Fitted curves (Fig. 2, *dotted line*) are close to the curves calculated with 5 parameter estimates, except for the lower curvature at the highest values of PFD [where the weights of the criteria function (Eq. 7) were higher].

Simplified analytical solutions (with 4 or 5 estimated parameters) compared to the initial dynamic model (Eq. 3) have the advantage of avoiding the initial condition problem for Y at t_0, Y_0, that occurs with any numerical integration method. In the case of the simplified model with 5 parameter estimates, at t_0, $I_0 = 0$, and the initial condition of the effective yield, Y_0, and its variance $V(Y_0)$, can be estimated from Eq. (6) as:

$$\hat{Y}_0 = \frac{\hat{p}_1 + 1}{\hat{p}_2 + 1} \quad , \quad \hat{V}\left(\hat{Y}_0\right) =$$

$$= \left(\frac{\hat{p}_1 + 1}{\hat{p}_2 + 1}\right)^2 \left(\frac{V(\hat{p}_1)}{(\hat{p}_1 + 1)^2} + \frac{V(\hat{p}_2)}{(\hat{p}_2 + 1)^2} - 2\frac{\hat{Cov}(\hat{p}_1, \hat{p}_2)}{(\hat{p}_1 + 1)(\hat{p}_2 + 1)}\right) \quad (10)$$

When I_t converges to infinity, the minimum effective yield, Y_{min}, and its variance $V(Y_{min})$ can be estimated from Eq. (6) by:

$$\hat{Y}_{min} = \frac{\hat{p}_1}{\hat{p}_2} \quad , \; \hat{V}\left(\hat{Y}_{min}\right) =$$

$$= \left(\frac{\hat{p}_1}{\hat{p}_2}\right)^2 \left(\frac{V(\hat{p}_1)}{\hat{p}_1{}^2} + \frac{V(\hat{p}_2)}{\hat{p}_2{}^2} - 2\frac{C\hat{o}v(\hat{p}_1, \hat{p}_2)}{\hat{p}_1\hat{p}_2}\right) \qquad (11)$$

And in the case of the simplified model with 4 parameter estimates, this becomes:

$$\hat{Y}_0 = \left(\hat{p}_2 + 1\right)^{-1}, \; \hat{V}\left(\hat{Y}_0\right) = \left(\frac{1}{\hat{p}_2 + 1}\right)^2 \left(\frac{V(\hat{p}_2)}{(\hat{p}_2 + 1)^2}\right),$$

$$Y_{min} = 0 \text{ and } V(Y_{min}) = 0 \qquad (12)$$

The results of these calculations are given in Table 4. In all cases, estimates of Y_0, within confidence intervals (CI) calculated from the standard error, [SE; CI = mean±1.96 SE, SE equal to the square root of the variance estimates $\hat{V}\left(\hat{Y}_0\right)$] remained below 1, the upper limit for the effective yield of photochemical energy conversion. Y_0 values estimated with the 5-parameter simplified model were close to Y_0 as estimated from the 4-parameter simplified model, even if they were, in all cases, significantly different. In addition, for the curves fitted with the 5-parameter equation (6), estimates of Y_{min} were small and the confidence intervals of Y_{min} included 0.

Demonstration and quantification of a cumulative effect of irradiation on photosystems: Estimates of k were significantly smaller than 1, implying that the irradiation history influenced the effective yield of photochemical energy conversion. As a qualitative demonstration of this process, Y_t decreased faster in the RLC experiments where diatoms were exposed to progressively increasing PFD, than for the second experiments, in which diatoms were kept in the darkness until the time t at which they were suddenly exposed to a given E_t for 50 s. A progressive but rapid increase of PFD decreases the photosynthetic performances of the plant. The characteristic time of this cumulative effect, which corresponds to the time scale of the residual photon accumulation, can be estimated as 1/k. In our study, the average characteristic accumulation time was estimated at 38 s (varying between 25 s and 102 s in the case of the 5-parameter model and between 20 s and 252 s in the case of the 4-parameter model, which had higher variance

Table 2. Example of correlation coefficients matrix estimates for parameters $\{\hat{k}, \hat{p}_1, \hat{p}_2, \hat{p}_3, \hat{p}_4\}$. k was less correlated to the other parameters estimates likely because of the optimisation procedure which consisted in calculating two different minimization criteria functions.

	k	p_1	p_2	p_3	p_4
k	1.00	0.35	0.36	−0.35	0.36
p_1	0.35	1.00	0.99	−0.99	0.99
p_2	0.36	0.99	1.00	−0.99	0.99
p_3	−0.35	−0.99	−0.99	1.00	−0.99
p_4	0.36	0.99	0.99	−0.99	1.00

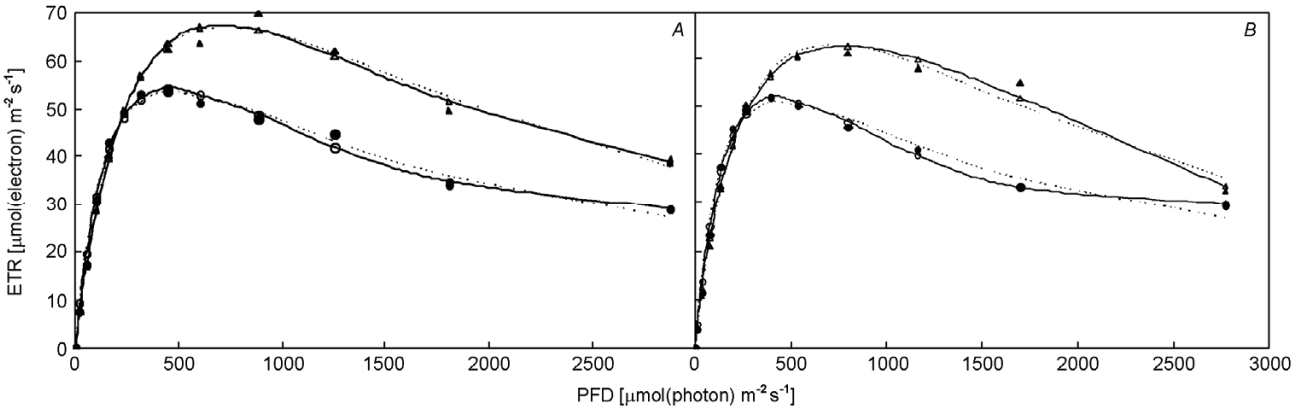

Fig. 2. Apparent electron transport rate (ETR) curves fitted by two cases: the RLC (*dots*) and the RC (*triangles*) measurements. *Solid symbols* represent the measured data and *open symbols* represent simulated values. *Solid lines* represent the fitted curves with 5 parameter estimates $\{\hat{k}, \hat{p}_1, \hat{p}_2, \hat{p}_3, \hat{p}_4\}$ and *dashed lines* represent the fitted curves with 4 parameter estimates $\{\hat{k}, \hat{p}_2, \hat{p}_3, \hat{p}_4\}$. Two concentrations in the biofilm were investigated: (*A*) 36±5 mg(Chl *a*) m^{-2}. (*B*) 53±7 mg(Chl *a*) m^{-2}. In all the cases, the models fitted well to the data and model simplifications (5 and 4 parameters) are significantly close. The main differences between RC and RLC curves were due to the residual effect of their irradiation history which provoked a sharper decrease of the effective yield and, hence, a lower maximum apparent ETR in RLC curves relative to RC.

Table 3. Best estimates and standard errors of parameter estimates $\{\hat{k}, \hat{p}_2, \hat{p}_3, \hat{p}_4\}$ using Eq. (8) in the calculation of ETR_t with $p_1 = 0$. Two concentrations were investigated: (*1*) 36±5 (SD, *n*=4) mg(Chl *a)* m^{-2} and (*2*) 53±7 (SD, *n*=4) mg(Chl *a*) m^{-2}, and two different irradiation dynamics were applied (corresponding to RLC and RC, respectively).

	RLC – 1		RC – 1		RLC – 2		RC – 2	
	Best estimates	SE	Best estimates	SE	Best estimates	SE	Best estimates	SE
k	$2.61\ 10^{-2}$	$0.83\ 10^{-2}$	$2.61\ 10^{-2}$	$1.05\ 10^{-2}$	$2.71\ 10^{-2}$	$0.69\ 10^{-2}$	$2.71\ 10^{-2}$	$1.18\ 10^{-2}$
p_2	$2.60\ 10^{-2}$	$0.00\ 10^{-2}$	$10.1\ 10^{-2}$	$0.00\ 10^{-2}$	$9.07\ 10^{-4}$	$0.01\ 10^{-4}$	$15.2\ 10^{-2}$	$0.00\ 10^{-2}$
p_3	$12.4\ 10^{-1}$	$0.00\ 10^{-1}$	$1.51\ 10^{-1}$	$0.00\ 10^{-1}$	$18.0\ 10^{-1}$	$0.00\ 10^{-1}$	$1.04\ 10^{-1}$	$0.00\ 10^{-1}$
p_4	$1.18\ 10^{-1}$	$0.00\ 10^{-1}$	$3.24\ 10^{-1}$	$0.00\ 10^{-1}$	$1.58\ 10^{-1}$	$0.00\ 10^{-1}$	$3.54\ 10^{-1}$	$0.00\ 10^{-1}$

Table 4. Best estimates and standard errors of parameter estimates $\{\hat{Y}_0, \hat{Y}_{min}\}$ calculated from the 5-parameters model (Eq. 8) and best estimates and standard errors of parameters estimates $\{\hat{Y}_0\}$ calculated from the 4-parameters model (Eq. 14). Two concentrations in the biofilm were investigated: (*1*) 36±5 (SD, *n*=4) mg(Chl *a*) m^{-2} and (*2*) 53±7 (SD, *n*=4) mg(Chl *a*) m^{-2}, and two different irradiation dynamics were applied (corresponding to RLC and RC, respectively).

	RLC – 1		RC – 1		RLC – 2		RC – 2	
	Best estimates	SE	Best estimates	SE	Best estimates	SE	Best estimates	SE
$Y_0(5)$	0.9524	$3.16\ 10^{-4}$	0.9567	$6.61\ 10^{-4}$	0.9629	$2.58\ 10^{-4}$	0.8661	$3.84\ 10^{-4}$
Y_{min}	0.0123	$8.55\ 10^{-3}$	–0.0148	$15.52\ 10^{-3}$	0.0086	$6.90\ 10^{-3}$	0.0064	$4.38\ 10^{-3}$
$Y_0(4)$	0.9669	$2.35\ 10^{-4}$	0.9082	$2.36\ 10^{-4}$	0.9987	$1.27\ 10^{-4}$	0.8680	$4.60\ 10^{-4}$

estimates). These quantitative results formally demonstrate that the time during which irradiation has a residual effect on photosystems is estimated at the scale of the minutes, and are consistent with previous experimental observations (Schreiber *et al.* 1997, Johnson 2000). A minimum of two curves is necessary to estimate k, but the estimates can be more accurate with more curves. In this perspective, the criteria function (Eq. 8) can be extended for the case of Q > 2 curves, each estimated with n_Q data:

$$\psi = \min\left[\sum_{q=1}^{Q}\sum_{i=1}^{n_q}\left(\left(\varphi_{Yq}\left(I_{ti}, \hat{\theta}_{Yq}\right) - \sum_{r=1}^{Q}\varphi_{Yr}\left(I_{ti}, \hat{\theta}_{Yr}\right)\right)0.5\beta E_{ti}\right)^2\right] \quad (13)$$

Ecophysiological implications of the model: For the sake of simplicity, the 4-parameter model (with $\{\hat{k}, \hat{p}_2, \hat{p}_3, \hat{p}_4\}$) remains the best approximation, and is particularly useful when only a small number of successive data are available (only 12 data points in the present case). Therefore, the recommended model approximation for describing the variations of ETR is:

$$ETR_t = 0.5\beta E_t\left(\frac{e^{\left(-aI_t^b\right)}}{c + e^{\left(-aI_t^b\right)}}\right) = 0.5\beta E_t\left(\frac{1 - Y_0}{Y_0 e^{\left(-aI_t^b\right)}} + 1\right)^{-1} \quad (14)$$

By analogy with PE curves (*e.g.* Jassby and Platt 1976, Platt *et al.* 1980), ecophysiologists used the slope at the origin and maximum of the electron transport rate (ETR_{max}) to estimate the photosynthetic efficiency and the photosynthetic capacity, respectively (Campbell *et al.* 2003, Silva and Santos 2003). In other studies, a photoinhibition term was added to take into account the downturn of the curve when the PFD increases (Longstaff *et al.* 2002, Hill *et al.* 2004, Ralph and Gademann 2005). The photosynthetic efficiency changes with the physiological state of the plants, and particularly its adaptation to the PFD received (Johnson 2000). The photosynthetic efficiency and photosynthetic capacity also vary with temperature and other environmental conditions (Johnson 2000, Campbell *et al.* 2003, Silva and Santos 2003).

However, our study attempts to show that in ETR calculations the interpretation of these parameters as a function of the environmental variability is not straightforward. We demonstrate that ETR variations are not only governed by PFD, E_t, but also by the dynamics of the effective yield, Y_t, which depends on the way that the plant perceived photons, described by the function, $I(\tau)$. As a consequence, the conditions under which the plant samples received different PFD (durations and irradiances) are fundamental to the determination of both the slope at the origin and the maximum value of the estimated ETR, ETR_{max}. Our results show that with the same E_t series applied to two identical plant samples, but with a different irradiation history (Fig. 2*A,B*), we obtained two different slope at the origin and ETR_{max} (Fig. 2).

The downturn of the curve, after ETR_{max} was reached, was always observed only because the effective yield

converges asymptotically to zero as E_t increases. This is confirmed by the fact that the derivative functions of Eqs. (6) and (14) have a null value for a positive PFD and is consistent with an estimated Y_{min} not significantly different from zero. As a consequence, ETR_{max} must be considered an optimum value defined for specific conditions of a highly fluctuating irradiation, but not, in any case, as a "photosynthetic capacity" (which is an eco-physiological property of the plant, regardless of the changes in PFD). In addition, the downturn of the curve, after ETR_{max} was reached, could not be interpreted in any case as a photo-inhibition process. What can be called a "short-term photo-inhibition" occurs as soon as dark-adapted plants are exposed to PFD, as shown by the decrease of F_m and F_o and the exponential decrease of the effective yield of photochemical energy conversion, Y_t (Johnson 2000).

Conclusion: Measures of the ETR are used to assess the physiological state of the plant (Riznichenko *et al.* 1996), and RLC experiments investigate the capacity of the plant to endure a stress (induced by irradiation and other environmental variables) and its recovery afterwards. The formulations described here for RLC and LC experiments are based on the calculation of the effective yield of photochemical energy conversion and electron transport rate as a function of a dynamic irradiation environment. In particular, the dynamic nature of the effective yield variations (Genty *et al.* 1989) includes an effect of residual irradiation history (Johnson 2000, Schreiber *et al.* 1997), and the proposed model described here is the first one designed to represent these dynamic characteristics explicitly. Variations in parameter estimates quantify explicitly the effect of integrated irradiation stresses, and more generally, the model formulation offers new perspectives for investigating dynamics of both photosynthetic yield and ETR, which are sensitive to short-term irradiation changes. This may include, with suggested changes of the model (3), *in situ* variations such as those recorded for marine benthic microalgal biofilms (Serôdio 2003) or for terrestrial plants submitted to sun flecks (Skillman and Winter 1997, Matsubara *et al.* 2005). The model described in this study can be used more widely to simulate the effect of any irradiation fluctuations, as long as they can be formulated in the "residual effect of irradiation" functions (Eq. 2). Therefore, the combination of controlled experiments and *in situ* measurements could now be used not only to determine the physiological state of the plant at the moment of measurement, but also reconstruct what were the past conditions of irradiation from a small number of successive measurements.

References

Blanchard, G.F., Guarini, J.M., Gros, P., Richard, P.: Seasonal effect on the relationship between the photosynthetic capacity of intertidal microphytobenthos and short-term temperature changes. − J. Phycol. **33**: 723-728, 1997.

Campbell, S., Miller, C., Steven, A., Stephens, A.: Photosynthetic responses of two temperate seagrasses across a water quality gradient using chlorophyll fluorescence. − J. Exp. Mar. Biol. Ecol. **291**: 57-78, 2003.

Consalvey, M., Jesus, B., Perkins, R.G., Brotas, V., Paterson, D.M.: Monitoring migration and measuring biomass in benthic biofilm: the effect of dark/far-red adaptation and vertical migration on fluorescence measurements. − Photosynth. Res. **81**: 91-101, 2004.

Dau, H.: Short-term adaptation of plants to changing light intensities and its relation to Photosystem-II photochemistry and fluorescence emission. − J. Photochem. Photobiol. B **26**: 3-27, 1994.

Figueroa, F.L., Conde-Alvarez, R., Gomez, I.: Relations between electron transport rates determined by pulse amplitude modulated chlorophyll fluorescence and oxygen evolution in macroalgae under different light conditions. − Photosynth. Res. **75**: 259-275, 2003.

Frenette, J.J., Demers, S., Legendre, L., Dodson, J.: Lack of agreement among models for estimating the photosynthetic parameters. − Limnol. Oceanogr. **38**: 679-687, 1993.

Genty, B., Briantais, J.-M., Baker, N.R.: The relationship between quantum yield of photosynthetic electron transport and quenching of chlorophyll fluorescence. − Biochim. Biophys. Acta **990**: 87-92, 1989.

Hewson, I., O'Neil, J.M., Dennison, W.C.: Virus-like particles associated with *Lyngbya majuscula* (Cyanophyta; Oscillatoriacea) bloom decline in Moreton Bay, Australia. − Aquat. Microb. Ecol. **25**: 207-213, 2001.

Hill, R., Schreiber, U., Gademann, R., Larkum, A.W.D., Khul, M., Ralph, P.J.: Spatial heterogeneity of photosynthesis and the effect of temperature-induced bleaching conditions in three species of corals. − Mar. Biol. **144**: 633-640, 2004.

Horton, P., Ruban, A.: Molecular design of the photosystem II light-harvesting antenna: photosynthesis and photoprotection. − J. Exp. Bot. **56**: 365-373, 2004.

Jassby, A.D., Platt, T.: Mathematical formulation of the relationship between photosynthesis and light for phytoplankton. − Limnol. Oceanogr. **21**: 540-547, 1976.

Johnson, Z.: Regulation of the Marine Photosynthetic Efficiency by Photosystem II. − PhD Thesis. Duke University. North Carolina 2000.

Kolber, Z., Falkowski, P.G.: Use of active fluorescence to estimate phytoplankton photosynthesis *in situ*. − Limnol. Oceanogr. **38**: 1646-1665, 1993.

Kubler, J.E., Raven, J.: Nonequilibrium rates of photosynthesis and respiration under dynamic light supply. − J. Phycol. **32**: 963-969, 1996.

Kühl, M., Glud, R.N., Borum, J., Roberts, R., Rysgaard, S.: Photosynthetic performance of surface associated algae below sea ice as measured with a pulse-amplitude-modulated (PAM) fluorometer and O_2 microsensors. − Mar. Ecol. Progr. Ser. **223**: 1-14, 2001.

Lichtenhaler, H.K.: The Kautsky effect. 60 years of chlorophyll fluorescence induction kinetics. − Photosynthetica **27**: 45-55, 1992.

Longstaff, B.J., Kildea, T., Runcie, J.W., Cheshire, A., Dennison, W.C., Hurd, C., Kana, T., Raven, J.A., Larkum, A.W.D.: An *in situ* study of photosynthetic oxygen exchange and electron transport rate in the marine macroalgae *Ulva lactuca* (Chlorophyta). − Photosynth Res. **74**: 281-293, 2002.

Lorenzen, C.J.: A method for the continuous measurement of *in*

vivo chlorophyll concentration. Deep Sea Res., **13**: 223-227, 1966

Matsubara, S., Naumann, M., Martin, R., Nichol, C., Rascher, U., Morossinotto, T., Bassi, R., Osmond, B.: Slowly reversible de-epoxidation of lutein-epoxide in deep shade leaves of a tropical tree legume may 'lock-in' lutein-based photoprotection during acclimation to strong light. − J. Exp. bot. **56**: 461-468, 2005.

Nedbal, L., Soukupova, J., Kaftan, D., Whitmarsh, J., Trtilek, M.: Kinetic imaging of chlorophyll fluorescence using modulated light. − Photosynth. Res. **66**: 3-12, 2000.

Nelder, V.A., Mead, R.: A simplex method for function minimization. − Computer J. **7**: 308-13, 1965.

Platt, T., Gallegos, C.L., Harrison, W.G.: Photoinhibition of photosynthesis in natural assemblages of marine phytoplankton. − J. Mar. Res. **38**: 687-701, 1980.

Ralph, P.J., Gademann, R.: Rapid Light Curve: A powerful tool to assess photosynthetic activity. − Aquat. Bot. **82**: 222-237, 2005.

Riznichenko, G., Lebedeva, G., Pogosyan, S., Sivchenko, M., Rubin, A.: Fluorescence induction curves registered from individual microalgae *cenobiums* in the process of population growth. − Photosynth. Res. **49**: 151-157, 1996.

Schreiber, U., Bilger, W., Neubauer, C.: Chlorophyll fluorescence as a non intrusive indicator for rapid assessment of *in vivo* photosynthesis. In: Schulze, E.-D., Caldwell, M.M. (ed.): Ecophysiology of Photosynthesis. Pp. 49-70. Springer-Verlag, Berlin 1994.

Schreiber, U., Schliwa, U., Bilger, W.: Continuous recording of photochemical and non-photochemical chlorophyll fluorescence quenching with a new type of modulation fluorometer. − Photosynth. Res. **10**: 51-62, 1986.

Schreiber, U., Gademann, R., Ralph, P.J., Larkum, A.W.D.: Assessment of photosynthetic performance of *Prochloron* in *Lissoclinum patella* in hospite by chlorophyll fluorescence measurements. − Plant Cell Physiol. **38**: 945-951, 1997.

Seddon, S., Cheshire, A.C.: Photosynthetic response of *Amphibolis antarctica* and *Posidonia australis* to temperature and dessication using chlorophyll fluorescence. − Mar. Ecol. Progr. Ser. **220**: 119-130, 2001.

Serôdio, J.: A chlorophyll fluorescence index to estimate short-term rates of photosynthesis by intertidal microphytobenthos. − J. Phycol. **39**: 33-46, 2003.

Serôdio, J., Vieira, S., Cruz, S., Coelho, H.: Rapid light-response curves of chlorophyll fluorescence in microalgae: relationship to steady-state light curves and non-photochemical quenching in benthic diatom-dominated assemblages. − Photosynth. Res. **90**: 29-43, 2006.

Silva, J., Santos, R.: Daily variation patterns in seagrass photosynthesis along a vertical gradient. − Mar. Ecol. Progr. Ser. **257**: 37-44, 2003.

Skillman, J.B., Winter, K.: High photosynthetic capacity in a shade-tolerant crassulacean acid metabolism plant: Implications for sunfleck use, nonphotochemical energy dissipation, and susceptibility to photoinhibition. − Plant Physiol. **113**: 441-450, 1997.

White, A.J., Critchley, C.: Rapid Light Curves: A new fluorescence method to assess the state of the photosynthetic apparatus. − Photosynth. Res. **59**: 63-72, 1999.

Wing, S.R., Patterson, M.R.: Effects of wave-induced light flecks in the intertidal zone on photosynthesis in the macroalgae *Postelsia palmaeformis* and *Hedophyllum sessile* (Phaephyceae). − Mar. Biol. **116**: 519-52, 1993.